Superhyperfine structures of the relaxed excited state of the *F* centers in KCl observed by zero-frequency optical detection of electron-nuclear double resonance

Norio Akiyama and Hiroshi Ohkura
Department of Electronic Engineering, Okayama University of Science, 1-1 Ridai-cho, Okayama 700, Japan
(Received 14 July 1995; revised manuscript received 30 November 1995)

The superhyperfine (shf) spectrum of the relaxed excited state (RES) of the *F* centers in KCl has been observed by detecting decrement dips of the quantum efficiency η_F of the *F* luminescence in its dependence on the magnetic field *B* below 0.31 T at 4 K. This method is called zero-frequency optical detection of electron-nuclear double resonance (ZF-ODENDOR) described earlier by the Jaccard group. The shf spectrum depends on the angle Φ between *B* and the crystalline axis. From curve-fitting analysis of its Φ dependence, the isotropic and anisotropic shf interaction constants (*a* and *b*) of the RES are determined up to the 32nd shell as a function of ρ being the shell distance from an anion vacancy divided by a lattice constant. From the ρ dependence of the *a* values, the envelope wave function (EWF) of the RES is estimated as a $|2s\rangle$-like EWF admixed with a small fraction (13%) of $|2p\rangle$-like EWF (Bogan and Fitchen's model). The amplification factors $A_+ = 819$ and $A_- = 950$, and an orbital extension constant $\eta = 0.65$ for the EWF are adopted. Thus, the advantage of the vibronic model of the RES, that is theoretical extension of Bogan and Fitchen's model, is supported. The ρ^{-3} dependence of the b_1 values is confirmed in the range $\rho > 3.5$.

I. INTRODUCTION

The investigation of the optically excited state (OES) in solids is one of the most attractive research fields not only for its academic interest but also for its industrial demand in optoelectronics. In particular, the study of the *F* centers in alkali halides can provide useful knowledge about the OES of defects with deep electronic levels coupled strongly with phonons in condensed matter. However, detailed electronic structure in the *lowest relaxed excited state* (RES) of the *F* centers has been left in debated question,[1] ever since Swank and Brown observed the anomalously long radiative lifetime of the RES in 1962.[2–4]

Two different models have been proposed for the RES. The first was proposed by Bogan and Fitchen[5] in 1970. It states that the RES consists of a $|2s\rangle$-like electronic wave function admixed by a small fraction of a $|2p\rangle$-like wave function energetically lying above through electron and phonon interaction (Bogan and Fitchen's model). Later, including its strong and intermediate interaction, the model has been sophisticated as a *vibronic model* by many authors including us.[6–12] Based on the vibronic model, the external perturbation (Stark,[5,13] stress,[14,15] magnetic field[16–20]) effects on the RES have been explained consistently. Now, Bogan and Fitchen's model is fundamentally equivalent to a two-level approximation of the vibronic model.[6–12] On the other hand, an alternative model had been proposed by Fowler[21] before Ref. 5. It shows that the RES consists of a spatially extended $|2p\rangle$-like wave function (*extended* $|2p\rangle$*-like model*). Although this model failed to explain the perturbation effects on the RES, particularly for the Stark effect, it still survived because of the sole experimental evidence deduced from the analysis of optical detection of electron-nuclear double resonance (ODENDOR) of the RES in KI and KBr.[22,23]

Later, Reyher *et al.*[24,25] measured the full width at a half maximum (FWHM) $\Delta B_{1/2}$ and the *g* shift of the electron spin resonance (ESR) line of the RES using OD of ESR (ODESR). They pointed out that the *g* shift of the RES could be more satisfactorily evaluated numerically if one adopts the widely spread $|2s\rangle$-like wave function for the RES in Ref. 25. Furthermore, Romanov *et al.*[26] observed the isotope effects in the $\Delta B_{1/2}$ for the ^{41}K-rich *F* centers. From their analysis they proposed that the RES consists of a *well-localized* $|2s\rangle$*-like wave function*.

The present work is aimed to complement the validity of the vibronic model of the RES by elucidating its wave function with a zero-frequency ODENDOR (ZF-ODENDOR) method, which was developed by Mezger and Jaccard.[27] The method is solely available for the crystals, which were colored rather densely. Suppose when the specimen was optically excited to the RES, it may make pair with a nearby lying *F* center in the ground state (GS) to form a distant pair (DP) temporarily.[28–30] In the Appendix, we briefly summarize a temporary pairing process (TPP) of DP and a working principle of ZF-ODENDOR associated with it. Actually, they observed the decrement dips at a certain magnetic field B_c in the magnetic field *B* dependence of the quantum efficiency η_F of the *F* center luminescence. They deduced that the dip corresponds to a ZF-ODENDOR signal that occurs when a nuclear Zeeman energy $g_n\mu_n B_c$ at the B_c for each nucleus is equal to one-half of its hyperfine (hf) coupling energy $W_{\rm hf}$ that is proportional to the nuclear magnetic moment including a factor of $g_n\mu_n$, where g_n is a nuclear *g* factor and μ_n is the nuclear Bohr magneton. Then they emphasized that B_c is independent of the isotope effect by nucleus.

As the envelope wave function (EWF) of the RES of the *F* centers is predicted to be widely spread, the $W_{\rm hf}$ for the *i*th nucleus surrounding the vacancy are different from each other. Hereafter, we may call them the superhyperfine (shf) interaction energy $W_{{\rm shf},i}$ for the *i*th nucleus. Similarly, we

call the B dependence of $B_{c,i}$ the shf spectrum for the ith nucleus. Thus, in accordance with the preceding paragraph, the $B_{c,i}$ is independent of isotope effect. This is different from usual ENDOR or ODENDOR spectrum analysis[1] in which the isotope effect would often contribute to an advantageous searching mark for the assignment of $W_{\rm shf}$ in the case when the line shape of spectrum is narrow. Lack of the isotope effect, however, would give another simplicity for the analysis of the ZF-ODENDOR spectrum. Using a computer-searching method for data fitting analysis of the shf spectrum plotted as a function of the angle Φ between B and the crystalline axis, we can determine suitable fitting parameters of a and b values.

Recently, we have proposed that the ZF-ODENDOR method is extensively applicable for detecting $W_{\rm shf}$ of the RES, because the working principle of ZF-ODENDOR for the GS can be applicable also for the RES in DP.[31] Using analytical procedures described in Sec. III A, we have determined the a and b values for the RES up to the 32nd shell. The probability electron density of the RES that is proportional to the square of the EWF of the RES is calculated from a values making a reasonable assumption on the amplification factors for each K and Cl nucleus. The EWF of the RES is plotted as a function of ρ, which is a ratio of the nuclear distance r from the center of an anion vacancy divided by a lattice constant d. From the ρ dependence of the EWF, we check the validity of Bogan and Fitchen's model of the RES described above, and discuss its advantage.

However, the isotope effect due to the quadrupole interaction q terms would appear in the ZF-ODENDOR shf spectrum in principle. Unfortunately, the line shapes of the ZF-ODENDOR for the RES are wider than those of the ENDOR spectrum for the GS, and are structureless. Thus, we have hardly observed their expected spectrum. The fact shows that their contribution is negligibly small in comparison with a and b values. In fact, Mollenauer and Baldacchini[22,23] did not analyze the quadrupole spectrum in their ODENDOR spectrum of the RES of F centers in KBr and KI, even if the quadrupole effects of the Br and I nucleus are more predominant than the Cl nucleus.

This work consists of the following sections. In Sec. II, we describe experimental details of the ZF-ODENDOR method and the experimental results obtained. In Sec. III, the detailed analysis to determine the EWF of the RES is described. Using the parameters determined for the EWF, we calculate the $\Delta B_{1/2}$ of the ODESR line of the RES, which is in reasonable agreement with some of experimental data determined by previous authors. The isotope effects in $\Delta B_{1/2}$ observed in Ref. 26 is also explained. In Sec. IV, we discuss the alternative model of the *extended* $|2p\rangle$ *wave function* that has been deduced from the analysis in Refs. 22 and 23. We also point out that b_1 values show a ρ^{-3} dependence in the range $\eta\rho \gg 1$, where η is an orbital extension constant for the EWF that is coincident with an approximate form derived by Gourary and Adrian for a limiting case in the GS.[32] Moreover, the neglect of quadrupole interaction in the present analysis of the RES is commented upon. Finally, we carefully check the effect of the exchange interaction due to DP of F centers, and concluded that it would not be included in our shf spectrum.

II. EXPERIMENT AND RESULTS

Specimens were additively colored KCl crystals; the typical concentration of the F centers N_F was approximately 1.6×10^{17} cm^{-3}. The sample was thermally quenched from 450 °C to room temperatures and then cooled to 4 K in total darkness after loading on a cryostat. With reference to several works by Jaccard and co-workers[28–30] and a review listed in the Appendix, we may expect that an abundant concentration of DP would be naturally introduced in the specimen. So we may apply the ZF-ODENDOR method to our specimens. The validity of the application of this method is partly endorsed by an experimental fact that the signal appears as a direction of decrement of η_F that is a specific property of DP (see Appendix).

In fact, we have measured precisely the decrement dips of η_F in its B dependence. The specimen is kept in He gas at about 4 K, so that the bubbling noise caused by evaporation of liquid He can be avoided. The excitation light is from a well stabilized halogen lamp (150 W) linked with a combination of filters (Schott KG5, KG3, GG475), and is modulated by a mechanical chopper (chopping frequency at 591 Hz). The luminescence intensity proportional to η_F is detected by a Ge photodetector (Hamamatsu B2538-01) with a filter (Schott RG1000). The sweeping speed of B is about 3 mT s^{-1}. Detected signals are amplified using a digital lock-in detector (EG&G 5208, time constant of 100 ms) synchronized with the mechanical chopper. The output digital signals and the corresponding digital values of B, which has been calibrated by a Hall sensor, are sent to a memory in a computer. With the use of the optical modulation method described above, the time spent for measurements is reduced to about 1/25 compared with the magnetic field modulation method[33] used previously.

For further improvement of the signal-to-noise ratio, the signal averaging technique is used. This succeeds in summing up four times more data at a fixed angle Φ than the previous method.[33] The shf spectrum is obtained in an integrated shape. A typical shf spectrum, that is, the B dependence of η_F ($|\Delta L|$; proportional to the change of luminescence intensity L), is plotted in Fig. 1 as a function of B parallel to [100]. The noise level is shown by a bar. Its intensity is plotted in Fig. 2 as a function of Φ (in the ordinates) varying from $-2.8°$ to $+48.3°$ and B (in the abscissa). Here, the angle Φ is varied by $0.7°$ intervals from the [100] to the [110] directions around the [001] axis. The main intense peaks of interest are shown by black shading.

The two spectra marked as K_{III}^{GS} and Cl_{IV}^{GS} in Fig. 1 are the same as those that have been already identified as the shf spectra at the 3rd and 4th shells in the GS through ZF-ODENDOR by Mezger and Jaccard.[27] After the analysis of the Φ dependence of these spectra, the shf parameters are found to be nearly coincident with the results for the GS obtained by stationary ENDOR methods done by many authors.[34–38] In our previous work,[33] we pointed out that a series of shf spectra that appeared in the B range below 0.15 T should belong to those for the GS at shells further than the 4th shell. Thereupon, we have proposed intuitively that most of the shf spectra observed above 0.15 T would originate from the RES. Notice that the same sorts of dips have been

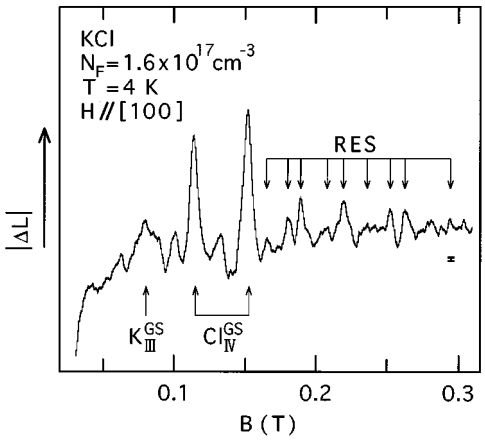

FIG. 1. The experimental trace of the change of the luminescence intensity $|\Delta L|$ of the F center in KCl at 4 K, namely the shf spectrum, is plotted as a function of magnetic field when $B \| [100]$. The bar shows noise level. The two spectra marked K_{III}^{GS} and Cl_{IV}^{GS} are the shf at the 3rd and 4th shells in the GS. The spectra observed in the magnetic field range above 0.15 mT correspond to that of the RES. Notice that $|\Delta L|$ is proportional to η_F.

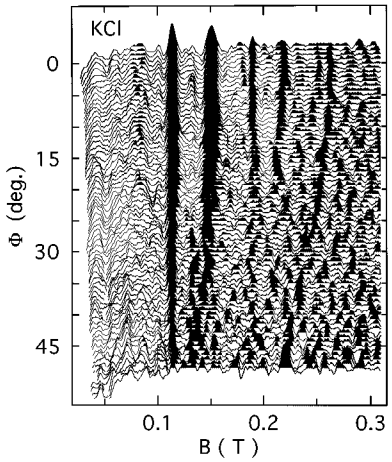

FIG. 2. The map of shf spectral intensity is plotted as a function of angle Φ. The main peaks of spectra are shown by black.

observed in Ref. 27. However, they did not mention their origins.

III. EXPERIMENTAL ANALYSIS

A. Analysis of the Φ dependence of the shf spectra

The main purpose of the present studies is to check the validity of the EWF of the RES of the F center in KCl proposed so far as an opponent model that consists of a $|2s\rangle$-like wave function including a small fraction (13%) of a $|2p\rangle$-like wave function.[5–12] Because of the quasispherical nature reflecting a mixing of the $2p$ state, we may safely assume that the symmetry around the vacancy is scarcely broken. This allows us to adopt the analytical forms of angular dependence of ZF-ODENDOR data for the RES to be the same as those of the ENDOR spectrum derived by Deigen *et al.*[34] and Kersten[37] for the GS. Although they derived the forms up to the 9th shell, we should derive them up to the 32nd shell in our demand. These forms are too complicated to be listed, partly in the interest of saving space.

In the present work, we assumed that the contribution of the q term would be negligibly small in comparison with the shf parameters. This assumption has been commonly adopted in the previous works on the magnetic resonance of the RES.[22–27] We will discuss the q terms in Sec. IV C.

The most important part of our fitting analyses of the shf spectrum is for the 2nd, 3rd, 4th, and 5th shells in the RES (Cl_{II}^{RES}, K_{III}^{RES}, Cl_{IV}^{RES}, and K_{V}^{RES}, respectively). Theoretical forms derived by Deigen *et al.*[34] for these nuclei are adopted for analysis. These fitting curves are plotted in Fig. 3(a) with solid lines; the fitting parameters are listed in Table I. The shf spectra for Cl_{IV}^{GS} and K_{III}^{GS} for the GS are also plotted in the same figure as a reference.[27,33] All lines show reasonably good fit to the corresponding main peaks in Fig. 2. From Table I, it is clearly found that the *a/h* value in the 5th shell is larger than that in the 3rd shell, while the *a/h* values in the 2nd and 4th shells are almost equivalent. This characteristic evidence allows us to adopt a working hypothesis that the RES consists of the $|2s\rangle$-like nature.

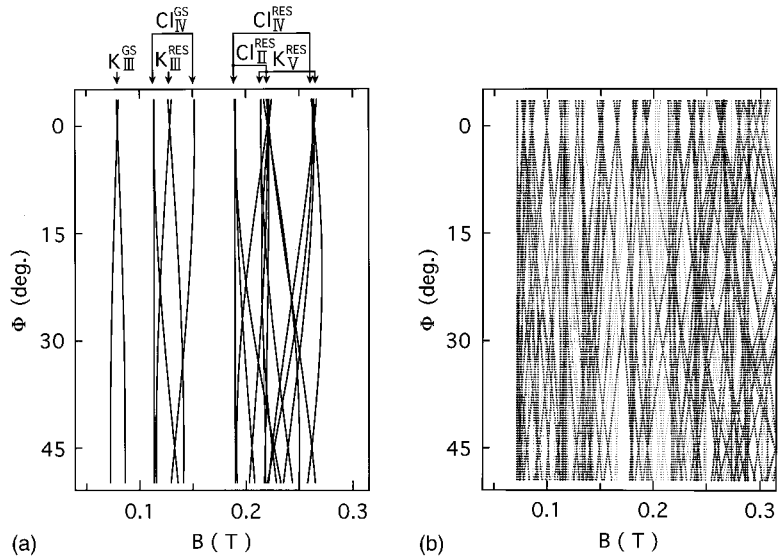

FIG. 3. (a) Fitting curves for the 2nd, 3rd, 4th, and 5th shells (Cl_{II}^{RES}, K_{III}^{RES}, Cl_{IV}^{RES}, and K_{V}^{RES}) in the RES are plotted with solid lines. Fitting curves for Cl_{IV}^{GS} and K_{III}^{GS} are plotted as a reference. (b) Additional fitting curves covering all shells are plotted. Fitting curves for K and Cl nuclei are plotted with thin and thick dotted lines, respectively.

TABLE I. Shf constants of the RES of F center in KCl determined from theoretical fitting of the Φ dependence of the shf spectrum. N values represent parameter ones that cannot be obtained from the theoretical reasons. The shells of the 7th, 15th, 23rd, 28th, and 31st are not present theoretically. $d^3|\Psi^*(\rho_i)|^2$ calculated from $(A_+, A_-)=(819,950)$ are listed in the last column.

Shell		Nucleus	a/h (MHz)	b_1/h (MHz)	b_2/h (MHz)	Θ (deg)	$d^3\|\Psi^*(\rho_i)\|^2$ ($\times 10^{-3}$)
2	[110]	^{35}Cl	1.756	0.166	0.002	N	0.896
3	[111]	^{39}K	0.510	0.052	N	N	0.634
4	[200]	^{35}Cl	1.786	0.203	N	N	0.912
5	[210]	^{39}K	0.927	0.075	0.001	6	1.154
6	[211]	^{35}Cl	(2.562)	(0.300)	(0.003)	(3)	1.308
9(a)	[300]	^{39}K	(1.333)	(0.187)	N	N	1.658
9(b)	[221]	^{39}K	(1.333)	(0.187)	(0.001)	(2)	1.658
11	[311]	^{39}K	(1.283)	(0.195)	(0.000)	(8)	1.596
13	[320]	^{39}K	(1.218)	(0.155)	(0.002)	(8)	1.514
14	[321]	^{35}Cl	(2.845)	(0.350)	(0.001)	(4)	1.452
16	[400]	^{35}Cl	(2.532)	(0.254)	N	N	1.293
17(a)	[410]	^{39}K	1.089	0.139	0.001	1	1.354
17(b)	[322]	^{39}K	1.089	0.139	0.001	1	1.354
18(a)	[330]	^{35}Cl	2.341	0.271	0.003	N	1.195
18(b)	[411]	^{35}Cl	2.341	0.271	0.003	2	1.195
19	[331]	^{39}K	0.994	0.124	0.001	0	1.237
20	[420]	^{35}Cl	1.897	0.212	0.002	1	0.968
21	[421]	^{39}K	0.810	0.100	0.002	0	1.007
22	[332]	^{35}Cl	1.775	0.131	0.003	2	0.906
24	[422]	^{35}Cl	1.353	0.161	0.002	2	0.691
25(a)	[500]	^{39}K	0.594	0.064	N	N	0.738
25(b)	[430]	^{39}K	0.594	0.064	0.002	2	0.738
26(a)	[510]	^{35}Cl	1.116	0.149	0.002	2	0.570
26(b)	[431]	^{35}Cl	1.116	0.149	0.002	2	0.570
27(a)	[333]	^{39}K	0.510	0.052	N	N	0.634
27(b)	[511]	^{39}K	0.510	0.052	0.001	2	0.634
29(a)	[520]	^{39}K	0.348	0.062	0.001	2	0.432
29(b)	[432]	^{39}K	0.348	0.062	0.001	2	0.432
30	[521]	^{35}Cl	0.804	0.118	0.001	3	0.410
32	[440]	^{35}Cl	0.676	0.083	0.001	N	0.345

Fitting curves are plotted in Fig. 3(b). This gives a reasonably good fit with Fig. 2. All fitting parameters are summarized in Table I for both ^{35}Cl and ^{39}K nuclei, respectively. The parameters Θ in the seventh column in Table I show deviation from axial symmetry defined in Ref. 34.

However, the available range of B for the shf spectrum is limited by our apparatus: The range is equivalent to the frequency (B) range between 0.963 MHz (50 mT) and 5.97 MHz (0.31 T) for ^{39}K, and between 0.417 and 2.59 MHz for ^{35}Cl, respectively. These limited ranges are shown by two bars in the right-hand side of Fig. 4. Because of such limitations of the B range, the parameter values of the 6th, 9th, 11th, 13th, 14th, and 16th shells were determined from partial fitting of the shf spectra. They are all listed in parentheses. Furthermore, the spectra of the 8th, 10th, and 12th shells for Cl nuclei could not be observed. The parameter values that do not appear from symmetry consideration are indicated by values of N. The spectra of the 7th, 15th, 23rd, 28th, and 31st shells do not exist from geometrical means.

B. Envelope wave function of the RES

Gourary and Adrian[32] have proposed that the a value at ρ_i, where ρ_i is a reduced distance of the ith nucleus at r_i divided by d, namely, $\rho_i = r_i/d$, is calculated as follows:

$$a(\rho_i) = C_i A_i |\Psi^*(\rho_i)|^2, \tag{1}$$

where C_i is a constant including the atomic magnetic values etc.,[38] A_i is an amplification factor, and $\Psi^*(\rho_i)$ is a normalized EWF at ρ_i. The quantity A_i was introduced to account for the oscillating character in $\Psi^*(\rho_i)$ caused by its orthogonalization with the core functions at the ith site.[32] If the values of A_i were known, the shape of $\Psi^*(\rho_i)$ could be calculated from experimental values of $a(\rho_i)$ with Eq. (1). In general, the A_i values may be different site by site i and are difficult to calculate theoretically.[25,38] The previous authors have adopted the empirical assumption that the A_i values for each cation A_+ are all the same and those for each anion A_- are also the same, although $A_+ \neq A_-$ in general.[22–24] With this assumption, the $\Psi^*(\rho_i)$ has been determined not

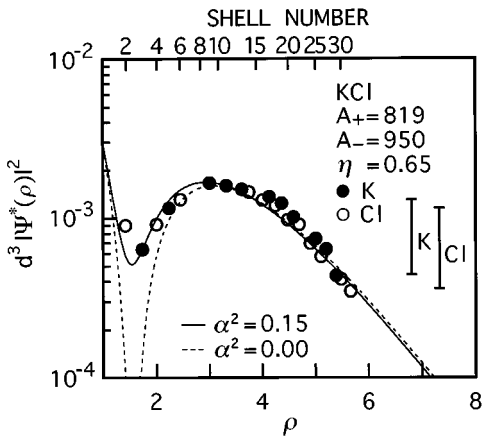

FIG. 4. The probability electron density $d^3|\Psi^*(\rho)|^2$ calculated from the isotropic shf constants a in Table I is plotted as a function of ρ with closed and open circles for anion and cation, respectively. $A_+=819$ and $A_-=950$ are adopted. The dotted lines are the $|2s\rangle$-like envelope wave function in Eq. (3) with $\eta=\eta_s=0.65$. The solid line is the best fit line of Eq. (4) with $\alpha^2=0.15$ and $\eta=\eta_s=\eta_p=0.65$. Two long bars at the right side show our observable experimental range for K and Cl nuclei.

only for the GS but for the RES, respectively.[22–24,27,34–37] Although Fowler and Kunz[39] discussed the validity of this assumption, we proceed to estimate $\Psi^*(\rho_i)$ by adopting the same assumption as was taken in the previous works, and leave the examination of Fowler and Kunz's claim for the future.

For convenience, we have taken up a well-used quantity for the ENDOR analysis: that is, a *probability electron density* $d^3|\Psi^*(\rho_i)|^2$, to find an electron fractionally in a unit cell with a volume d^3 sited at ρ_i from Eq. (1); it is shown as follows:

$$d^3|\Psi^*(\rho_i)|^2=a(\rho_i)d^3/(C_iA_i). \tag{2}$$

When we tentatively plotted them as a function of ρ_i, we found that their histogram showed an envelope with seemingly discontinuous shape. However, with adopting that $A_+/A_-=0.86$, we can transform them, particularly in the range of $\rho\gg3$, into a continuously varying smooth form plotted as a function of $\rho(=r/d)$. Adopting the working hypothesis introduced in the preceding subsection, we approximate this form as a part of $|2s\rangle$-like EWF, and then reduced it into the following normalized form[40] $\Psi^*_{2s}(\rho)$ by adjusting the value of either A_+ or A_-,

$$d^3|\Psi^*_{2s}(\rho)|^2=(1/\pi)\,\eta_s^3(1-\eta_s\rho)^2\exp(-2\,\eta_s\rho), \tag{3}$$

where η_s is an orbital extension constant and is estimated to be 0.65 by checking empirically from a node at $\eta_s\rho=1$. Now, by carefully checking the coincidence of estimated values in Eq. (2) with Eq. (3), the adjusted values of $(A_+,A_-)=(819, 950)$ are chosen. Thus determined values of $d^3|\Psi^*(\rho_i)|^2$ are summarized in the last column in Table I. They are also plotted in Fig. 4 as a function of ρ with closed and open circles for the K and Cl nuclei, respectively. Equation (3) is also plotted with dotted lines in the same figure. It shows good agreement in the region $\rho\gg3$ with $d^3|\Psi^*(\rho_i)|^2$ obtained experimentally.

In a small region of $\rho<3$ in Fig. 4, however, the dotted lines of Eq. (3) are seemingly much deviated from the experimental values. This discrepancy can be solved by adopting Bogan and Fitchen's model for the EWF of the RES $\Psi^*_{\rm RES}(\rho)$, which consists of a combination of $\Psi^*_{2s}(\rho)$ with a small fraction of the $|2p\rangle$-like EWF $\Psi^*_{2p}(\rho)$ with a mixing parameter of α.[5,9,10] Thus the modified probability electron density is shown as

$$d^3|\Psi^*_{\rm RES}(\rho)|^2=(1+\alpha^2)^{-1}[d^3|\Psi^*_{2s}(\rho)|^2+\alpha^2d^3|\Psi^*_{2p}(\rho)|^2], \tag{4}$$

where $d^3|\Psi^*_{2p}(\rho)|^2$ is presented as

$$d^3|\Psi^*_{2p}(\rho)|^2=(3\pi)^{-1}\eta_p^3(\eta_p\rho)^2\exp(-2\,\eta_p\rho), \tag{5}$$

with the orbital extension constant of η_p. Equation (5) is the same form as was adopted in Refs. 22 and 23.

The calculated value of Eq. (4) is plotted in Fig. 4 with solid line by adopting $\alpha^2=0.15$ and assuming $\eta=\eta_s=\eta_p=0.65$. This shows that the RES consists of $|2s\rangle$-like EWF mixed with 13% of $|2p\rangle$-like EWF. We point out that the value of α^2 determined is coincident with that determined previously by Imanaka *et al.* based on a two-level approximation of the vibronic model.[6–12]

Let us compare the determined value of $(A_+,A_-)=(819,950)$ with theoretical values that have been calculated by Reyher *et al.*[25] They have estimated the values of (A_+,A_-) as (580,740) for the cases of orthogonalized core functions, and as (700,810) for the relativistic core functions, respectively.

Finally, we discuss the value of $\eta=0.65$. This value is much smaller than $\eta=2.45$ for the GS in the F center in KCl.[38] The difference reveals that the EWF of the RES has larger orbital extension than that of the GS. This evidence endorses the previous proposal done by many authors from different experimental methods.[22–25] Recently, from the study of the resonant secondary radiation of F centers, we have anticipated that the orbital of the OES of F centers begins to spread immediately after the optical absorption.[41–43]

C. The half-width of ODESR line

We have derived the following form of $\Delta B_{1/2}$ from Eq. (4) in the same manner as it was derived by Reyher *et al.*:[24]

$$(\Delta B_{1/2})^2=[4.02\times10^{-5}(A_+/A_-)^2+1.63\times10^{-4}]\times(A_-)^2\eta^3(1+\alpha^4)/(1+\alpha^2)^2, \tag{6}$$

in units of mT, assuming $\eta=\eta_s=\eta_p$. Here, the form of $(\Delta B_{1/2})^2$ under the condition of $\alpha^2\gg1$ and $(A_+,A_-)=(650,1500)$ for the GS is equivalent to Eq. (11) with Eq. (13) in Ref. 24. With Eq. (6), the value of $\Delta B_{1/2}$ can be estimated to be 6.1 mT for $\alpha^2=0.15$ and 6.9 mT for $\alpha^2=0$. These values are nearly equal to some experimental data of $\Delta B_{1/2}$ summarized in the fourth column in Table II where their references are listed. The scattering of experimental values is caused by the difficulty in the artificial separation of $\Delta B_{1/2}$ of the GS and RES because of their very close g factors.

TABLE II. The values of the ODESR linewidth (FWHM) $\Delta B_{1/2}$ calculated from Eq. (6) using $A_+=819$, $A_-=950$, and $\eta=0.65$ in the cases when $\alpha^2=0.15$ and 0 are shown together with experimental values and their references.

Sample	α^2	$\Delta B_{1/2}$ Calc. (mT)	$\Delta B_{1/2}$ Expt. (mT)	Reference
			8.3 ± 2.0	24
			7.9	51
KCl	0.15	6.1	6.0 ± 0.3	46
	0	6.9	5.8 ± 0.2	26
			5.5 ± 2	50
^{41}KCl	0.15	5.7	5.4 ± 0.2	26
	0	6.5		

Finally, based on the present scheme, we have examined the isotope effects of $\Delta B_{1/2}$ that had been observed as 5.4 mT by Romanov *et al.*[26] (see Table II). By taking account of the isotope nature, the form of $\Delta B_{1/2}$ for ^{41}KCl is deduced by simply replacing the factor of 4.02×10^{-5} in Eq. (6) with 1.27×10^{-5}. Then, with introducing $\alpha^2=0.15$ into Eq. (6), the value of $\Delta B_{1/2}$ is calculated as 5.7 mT, which is close to the experimental value. On the other hand, $\Delta B_{1/2}$ is calculated as 6.5 mT for $\alpha^2=0$. The latter value is much deviated from their observation. The value of the ratio $\Delta B_{1/2}(^{41}\mathrm{KCl})/\Delta B_{1/2}(^{39}\mathrm{KCl})$ is calculated to 0.94 and 0.93 for $\alpha^2=0$ and $\alpha^2=0.15$, respectively. They are almost coincident with the experimental value of $\Delta B_{1/2}(^{41}\mathrm{KCl})/\Delta B_{1/2}(\mathrm{KCl})=0.93$ obtained by Romanov *et al.*[26] These results strongly endorse the validity of the present scheme.

IV. DISCUSSION

The present work is devoted to finding a consistent model for the RES of the F centers by clearing up a point of debate between the vibronic model[6–12] and the alternative model specified by an extended $|2p\rangle$-like EWF model.[21–23] In Sec. IV A, we find evidence to support the former scheme by comparing with the latter scheme, which was derived from the ODENDOR result for KI and KBr. In Sec. IV B, we show an empirical ρ^{-3} dependence of b_1 values in the region of $\eta\rho\geqslant2.6$. In Sec. IV C, we comment upon the quadrupole interaction for the RES. In Sec. IV D, we examine that the exchange effects due to DP or closed pairs (CP) of the F centers would not be included in our shf spectrum whether they are observed or not.

A. Alternative model of the RES: $|2p\rangle$-like EWF

In Refs. 22 and 23, it was proposed that the RES of F centers in KI and KBr would solely consist of a widely spread $|2p\rangle$-like EWF having the same form as Eq. (5) with the orbital extension constants $\eta_p=0.515$ and 0.48, respectively. However, in their ODENDOR analysis, they have resolved solely the shf constants within a limited region of $(\eta_s\rho,\eta_p\rho)\geqslant1$ where both forms of $|2s\rangle$-like and $|2p\rangle$-like EWF, which are as shown in Eqs. (3) and (5), are asymptotically reduced to an equivalent form if $\eta=\eta_p=\eta_s$. Thus, it would be hard to distinguish the $2s$ and $2p$ nature from their analysis. In order to clarify the $|2s\rangle$-like nature in the EWF, one should be careful to examine the shf constants for both models in the range of $(\eta_s\rho,\eta_p\rho)\leqslant1$, where the difference appears distinctly. In the present work, we have picked up the shf constants in this range from the analysis of the Φ dependence of the shf spectrum; the result is shown in Figs. 2 and 3(a). The node of the EWF plotted at the low range of ρ in Fig. 4 is convincing evidence to support the $|2s\rangle$-like model for the RES, which is basically Bogan and Fitchen's model.

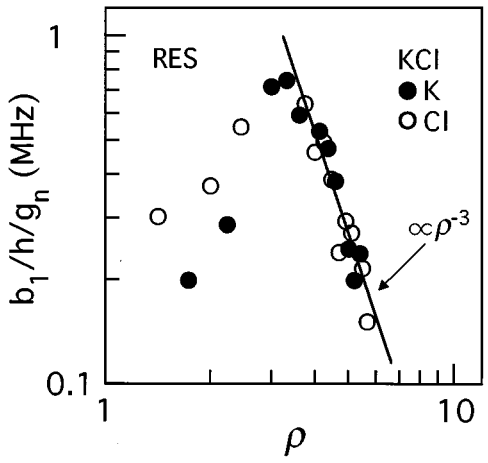

FIG. 5. The anisotropic shf constant normalized by the nuclear g factor $(b_1/h)/g_n$ are plotted against ρ. The solid line reveals a ρ^{-3} dependence.

Recently, we have measured the Φ dependence of shf spectrum for the RES of the F centers in both KBr and KI,[31,44] and determined the shf parameters for them. With using these parameters and considering the difference of resonant conditions for the ODENDOR and ZF-ODENDOR, we succeeded in reproducing the ODENDOR spectrum. It is almost the same as was reported in Refs. 22 and 23. This shows that Eq. (4) is still valid to describe Bogan and Fitchen's model of the RES in KBr and KI. The details of this work will be published elsewhere.

B. Anisotropic shf interaction of the RES

The b_1 values for each nucleus originate from the magnetic dipole-dipole interaction between the unpaired F electron and surrounding nuclei. The values of $(b_1/\mathrm{h})/g_n$ calculated from Table I are plotted in Fig. 5 as a function of ρ. The solid lines show a ρ^{-3} tendency in the range of $\rho\geqslant3.5$. Gourary and Adrian[32] derived an approximate form of b_1 for the GS in the case when the EWF is rather well localized. Their form reveals that b_1 is proportional to $|\delta\Psi^*(\rho)/\delta\rho|^2$, which is deduced to the ρ^{-3} dependence in the range of $\eta\rho>1$.

However, particularly at the ρ range lower than 3.5, the experimental points for the RES are deviated from ρ^{-3} dependence. This discrepancy reveals that the assumption adopted by Gourary and Adrian would be unreasonable in this range. Spaeth, Niklas, and Bartram,[45] have argued that

the form of b is generally divided into three parts depending on the degree of localization of the EWF. Possibly, in the case of a well-spread wave function such as the RES, one needs a different approach such as the linear combination of atomic orbitals approximation. However, we will leave such a theoretical calculation at the low ρ range for the future.

Let us evaluate the validity of the analytical forms derived by Deigen *et al.*[34] to estimate the b values. Although they derived them by means of the first-order perturbation theory, Kersten[37] derived them by means of second-order perturbation. However, the ratio of b_1/a values estimated from both schools for the GS up to the 9th shell are almost the equal amounts. Most of them are less than 23.5%; exceptions are 22.2% and 28.7% for the 8th and 14.0% and 19.7 % for the 9th shells by Deigen *et al.* and Kersten, respectively. This partially implies that the second-order correction would not be necessary for the present fitting analysis of the shf constants. On the other hand, the b_1/a values for the RES estimated from Table I are all accounted as less than 15.2%, with exception of 17.8% of the 29th shell. This evidence allows us to adopt the form of Deigen *et al.* for our analysis.

C. Quadrupole interaction

We discuss the reason we have neglected the q terms in our ZF-ODENDOR analysis. For ordinary ENDOR analysis of the GS, the q terms were useful in identifying the ENDOR spectrum in the case when they were small in comparison with the b value,[34,37] and their line shapes of the ENDOR spectrum were comparatively sharp. The different angular dependence from the shf spectrum is also helpful for distinction. On the contrary, the ZF-ODENDOR spectrum observed in the present study is usually structureless and has a wider line shape than that for ENDOR of the GS. Thus, it would make distinction difficult. As the linewidth of ENDOR of the F center has not been studied either for the GS or for the RES yet, theoretical corporation to improve experimental preciseness would be hopeless. This might be one of the reasons why Mollenauer and Baldacchini[22,23] have not analyzed the q term in the RES for KBr and KI, even if the Br and I nuclei have larger q terms than Cl.

Even so, we tried tentatively to include a small amount of q values in the analytical forms by considering occurrence probability. This addition gave little better fitting for the shapes of several shf lines. However, it would be hard to determine these values precisely with this means, except for qualitative estimation that $b>q$. Furthermore, we have failed in computer-aided analysis to fit the whole spectrum by tentatively adopting appropriately large q values. At any rate, our assumption to neglect the q terms is partly supported by these two unfavorable empirical facts.

There might be a possibility that the q values due to the nearest-neighboring (nn) sites would be large because of electric field due to the $2s$ electron density populated at the vacancy. If this is really true, we suspect that these spectra would be possibly buried as one of the unresolved lines at a higher magnetic range in the ZF-ODENDOR spectrum. However, our fitting effort using usual angular dependence forms was not successful. On the other hand, judging from relatively small b values estimated at the nn sites as shown in Fig. 5 and Table I, there might be an alternative idea that the effect of the $\langle r^{-3}\rangle$ term in the q values would not be desirable enough from a theoretical viewpoint. As a whole, the origin of both b and q values at the nn site is unexplored yet, and left for the future.

Generally speaking, theoretical determination of q and b values could not have been achieved unless all wave functions of the F center are well established. Comprehension of the EWF would be a milestone for this investigation.

D. Possibility of an exchange interaction

As was reviewed in the Appendix, when rather densely colored alkali halide crystals are optically excited, at least two types of *temporarily pairing of F* centers would occur under certain conditions. They are distinguished as distant and closed pairs (DP and CP) depending on the pairing distance. As was mentioned in Sec. II, we analyzed the present data by solely considering DP because our specimens are moderately colored. However, several experimental data caused by the exchange effect in CP as well as DP have been reported in the ODESR measurements.[46–48] For example, Murayama, Morigaki, and Kanzaki[46] and Mezger and Jaccard[47] observed the exchange effect in the ODESR spectrum of DP of the F centers in KCl. In the following paragraphs, we examine two limiting cases of strong and weak exchange effect that might appear in the shf spectrum.

When the exchange energy J exceeds the total shf energy and the Zeeman energy of $(g_e-g_e^*)\mu_e B$, where g_e and g_e^* are the electronic g values in the GS and the RES, respectively, we estimate qualitatively that the exchange effect may appear at a much higher magnetic field region than the range of the shf spectrum. However, this would be out of the detection limit of our apparatus. Thus, the strong exchange effect can be excluded.

In the case when J can be treated as a weak interaction, we can calculate the shf spectrum for DP, in a similar manner to that proposed by Jaccard, Schnegg, and Aegerter,[49] for the exchange effect of CP. The result shows that it may occur at B_c of $(a_i^2+4J^2)^{1/2}/(2g_{n,i}\mu_{n,i})$, where a_i is the isotropic shf constant in the ith nucleus. This predicts that the shf spectrum may appear characteristically at slightly but regularly shifted positions (several mT) from the spectrum obtained for $J=0$. Moreover, they show the same periodical Φ-dependence pattern in the B dependence as that of the fundamental shf spectrum. However, we could not find any such evidences in our experimental data of Fig. 2.

As a whole, we are convinced that the exchange effects would not be included in the present ZF-ODENDOR data.

V. CONCLUSION

By means of zero-frequency optical detection of ENDOR (ZF-ODENDOR) described by the Jaccard group, we have detected the superhyperfine (shf) interaction spectrum particularly for the relaxed excited state (RES) of the F centers

in KCl specimen, which was moderately colored so that a large fraction of distant F center pairs (DP) can be expected to exist. From the curve fitting analysis of the shf spectrum as a function of the angle Φ between the magnetic field and the crystalline axis, the isotropic and anisotropic shf constants of the RES of the F centers are determined separately up to the 32nd shell surrounding the anion vacancy. Because of nearly spherical symmetry of envelope wave function (EWF), we are allowed to adopt an analytical form derived by Deigen *et al.* for ENDOR analysis of the ground state (GS). These values are summarized in Table I. No convincing data of the quadrupole effect in the RES was obtained. Thus, we may assume that they are negligibly small. In order to picture the EWF for the RES from the isotropic shf interaction constant a values, we assumed that the amplification factors for cations and anions (A_+ and A_-) are all the same, although they are different from each other ($A_+ \neq A_-$). The EWF for the RES is estimated to have the form of Eq. (4). It reveals that the $|2s\rangle$-like EWF is admixed with a small fraction of about 13% of $|2p\rangle$-like EWF. Here, $(A_+, A_-) = (819, 950)$ and an orbital extension constant $\eta = 0.65$ have been adopted. This is fundamentally equivalent to Bogan and Fitchen's model,[5] which corresponds to a two-level approximation of the vibronic scheme of the RES.[6–12] The half width of ODESR line of the RES $\Delta B_{1/2}$ that was calculated using these parameters determined is in reasonable agreement with the experimental data. Two alternative models of the RES for EWF, which are a well-localized $|2s\rangle$-like wave function proposed by Romanov *et al.*[26] and an extended $|2p\rangle$-like wave function by Mollenauer and Baldacchini,[22,23] are compared with the present model. They are not satisfactory to explain the ZF-ODENDOR data and other experimental data of the RES as well. Therefore, the validity of the vibronic model of the RES has been supported.

ACKNOWLEDGMENTS

We are much obliged to Professor J.-M. Spaeth, Professor A. M. Stoneham, Professor U. M. Grassano, Dr. G. Baldacchini, Professor P. G. Baranov, Dr. N. G. Romanov, and Dr. H.-J. Reyher, for showing much interest and giving useful comments. Many thanks are due to Professor G. A. Williams in the University of Utah for careful reading of the original draft and giving valuable advice. Final thanks are due to Professor Y. Mori and Professor T. Iida in Osaka City University for continuing deep interest on this work. We thank S. Tahara and T. Iwao for experimental help.

APPENDIX: PRINCIPLES OF ODENDOR AND ZF-ODENDOR OF THE RES OF THE *F* CENTERS IN THEIR TEMPORARILY COUPLED PAIR

We summarize briefly the outline of previous works that are beneficial to understanding the present work of ZF-ODENDOR. Immediately after an electron in an F center is excited optically, its orbital begins to spread widely during lattice relaxation until thermalized at the RES.[31,41–43] In a rather densely colored crystal, the thermalized RES may undergo a temporarily pairing process (TPP) with a nearby lying isolated F center in the GS to form an F' center leaving an anion vacancy behind. Thereafter, the electron in the F' center would tunnel back to the anion vacancy nonradiatively to leave the F center behind, thus recovering two original F centers in the GS nonradiatively, so that it leads to a decrease of the quantum efficiency η_F of the F center luminescence. Such a quenching of η_F was observed by Miehlich[52] when the N_F exceeds approximately more than 1×10^{17} cm^{-3}.[28,48] Thereafter, Porret and Lüty observed the recovery of concentration-quenched η_F by raising the B applied (the Porret-Lüty effect).[29] They explained this effect by considering the spin symmetry in the TPP. With raising the B, two electrons (in the RES and GS) that would undergo TPP in the absence of B would tend to align to the B direction: A spin triplet is formed at the expense of a singlet. This prohibits TPP from forming a temporary triplet state because of the Pauli principle. So the occurrence of the nonradiative process is interrupted. This gives rise to enhancement of η_F.

On the basis of the Porret-Lüty effect, the ODESR method has been developed by several authors.[30,46,53] Suppose, if sending a resonant microwave to the electron Zeeman system that is sited either in the GS or the RES in TPP, it induces the transition from triplet to singlet at a resonant magnetic field B_c, thus resulting in the decrement of η_F in its B dependence. With this procedure, the ODESR signals of the GS and RES for the F and F_A centers were detected optically.

This working principle of ODESR can be applied extensively to the electron Zeeman system either in the GS or RES that are coupled with surrounding nuclei by the shf interaction energy $W_{\rm shf}$. At first, Mezger and Jaccard[27] pointed out that the decrement of η_F can be observed at B_c in its B dependence when the $W_{\rm shf}$ at a finite spin state $\pm(1/2)$ in the GS becomes equal to the nuclear Zeeman energy at B_c, when B is varied slowly. Thus, the shf spectrum for the GS can be detected without sending resonant electromagnetic field. This is a working principle of ZF-ODENDOR.[54] In the present work, we have shown that $W_{\rm shf}$ in the RES can be also detected, on the basis of the same principle.

Jaccard *et al.*[28,30,48] proposed that there might exist two sorts of TPP depending on the mean distances between both initial F centers. They are called the distant pairs (DP) and closed pairs (CP), which are roughly distinguished by the mean critical distances of 8 nm and 2–4 nm, respectively. DP and CP are experimentally distinguished by checking the direction of variation of η_F in the ODESR spectrum. Namely, a decrement of η_F is observed for the DP and an increment for CP. Jaccard, Schnegg, and Aegerter[49] showed that the exchange effect in CP would give rise to a different ESR spectrum from DP. Judging from the N_F contained in our specimen, we may expect that the abundant fraction of DP can exist. The expectation is endorsed by the experimental fact that the ZF-ODENDOR signals are in the direction of the decrement of η_F. This implies that we could hardly observe exchange effects in our ZF-ODENDOR spectrum.

[1] See, e.g., J.-M. Spaeth and F. Lohse, J. Phys. Chem. Solids **51**, 861 (1991).
[2] R. K. Swank and F. C. Brown, Phys. Rev. Lett. **8**, 10 (1962).
[3] R. K. Swank and F. C. Brown, Phys. Rev. **130**, 34 (1963).
[4] G. Spinolo and F. C. Brown, Phys. Rev. **138**, A450 (1964).
[5] L. D. Bogan and D. B. Fitchen, Phys. Rev. B **1**, 4122 (1970).
[6] F. S. Ham, Phys. Rev. B **8**, 2926 (1973).
[7] F. S. Ham and U. Grevsmühl, Phys. Rev. B **8**, 2945 (1973).
[8] Y. Kayanuma and Y. Toyozawa, J. Phys. Soc. Jpn. **40**, 355 (1976).
[9] Y. Kayanuma, J. Phys. Soc. Jpn. **40**, 363 (1976).
[10] K. Imanaka, T. Iida, and H. Ohkura, J. Phys. Soc. Jpn. **43**, 519 (1977).
[11] K. Imanaka, T. Iida, and H. Ohkura, J. Phys. Soc. Jpn. **44**, 1632 (1978).
[12] K. Iwahana, T. Iida, and H. Ohkura, J. Phys. Soc. Jpn. **47**, 599 (1979).
[13] H. Ohkura, K. Imanaka, O. Kamada, Y. Mori, and T. Iida, J. Phys. Soc. Jpn. **42**, 2137 (1976).
[14] R. E. Hetric and W. D. Compton, Phys. Rev. **155**, 649 (1967).
[15] N. Akiyama, K. Asami, M. Ishiguro, and H. Ohkura, J. Phys. Soc. Jpn. **50**, 3427 (1981).
[16] G. Baldacchini, U. M. Grassano, and A. Tanga, Phys. Rev. B **16**, 5570 (1977).
[17] G. Baldacchini, U. M. Grassano, and A. Tanga, Phys. Rev. B **19**, 1283 (1979).
[18] H. Ohkura, K. Tara, N. Akiyama, K. Iwahana, and Y. Mori, J. Phys. Soc. Jpn. **51**, 3615 (1982).
[19] H. Ohkura, Cryst. Lattice Defects Amorph. Mater. **12**, 401 (1985).
[20] N. Akiyama and H. Ohkura, Phys. Rev. B **40**, 3232 (1989).
[21] W. B. Fowler, in *Physics of Color Centers*, edited by W. B. Fowler (Academic, New York, 1968), Chap. 2.
[22] L. F. Mollenauer and G. Baldacchini, Phys. Rev. Lett. **29**, 465 (1972).
[23] G. Baldacchini and L. F. Mollenauer, J. Phys. (Paris) Colloq. **34**, C9-141 (1973).
[24] H. J. Reyher, K. Hahn, Th. Vetter, and A. Winnacker, Z. Phys. B **33**, 357 (1979).
[25] H. J. Reyher and A. Winnacker, Z. Phys. B **45**, 183 (1982).
[26] N. G. Romanov, Yu. P. Veshchunov, V. A. Vetrov, and P. G. Baranov, Phys. Status Solidi B **110**, 89 (1982).
[27] A. Mezger and C. Jaccard, Phys. Lett. A **79**, 118 (1980).
[28] C. Jaccard and M. Ecabert, Phys. Status Solidi B **87**, 497 (1978).
[29] F. Porret and F. Lüty, Phys. Rev. Lett. **26**, 843 (1971).
[30] C. Jaccard, Y. Ruedin, M. Aegerter, and P. A. Schnegg, Phys. Status Solidi B **50**, 187 (1972).
[31] N. Akiyama, Y. Mori, and H. Ohkura, in *Proceedings of the XII International Conference on Defects in Insulating Materials, Nordkirhen, 1992*, edited by O. Kanert and J.-M. Spaeth (World Scientific, Singapore, 1993), Vol. 1, pp. 114–116.
[32] B. S. Gourary and F. J. Adrian, in *Solid State Physics*, edited by F. Seitz and D. Turnbull (Academic, New York, 1960), Vol. 10.
[33] N. Akiyama, Y. Mori, H. Hanzawa, and H. Ohkura, J. Phys. Soc. Jpn. **58**, 2268 (1989).
[34] M. F. Deigen, M. A. Ruban, S. S. Ishchenko, and N. P. Baran, Zh. Éksp. Teor. Fiz. **51**, 1014 (1966) [Sov. Phys. JETP **24**, 676 (1967)].
[35] H. Seidel, Z. Phys. **165**, 218 (1961).
[36] W. C. Holton and H. Blum, Phys. Rev. **125**, 89 (1962).
[37] R. Kersten, Phys. Status Solidi B **29**, 575 (1968).
[38] H. Seidel and H. C. Wolf, in *Physics of Color Centers*, edited by W. B. Fowler (Academic, New York, 1968), Chap. 8.
[39] W. B. Fowler and A. B. Kunz, Phys. Status Solidi **40**, 249 (1970).
[40] Mollenauer and Baldacchini (Refs. 22 and 23) presented the probability density $d^3|\Psi^*(\rho)|^2$ as $P(\rho)$. On the other hand, Reyher *et al.* presented it as $|\tilde{\Psi}(\rho)|^2$, where $\tilde{\Psi}(\rho)$ is called the *reduced wave function* in Ref. 24.
[41] Y. Mori and H. Ohkura, J. Phys. Chem. Solids **51**, 663 (1990).
[42] N. Akiyama and H. Ohkura, J. Lumin. **60&61**, 713 (1994).
[43] N. Akiyama, F. Nakahara, and H. Ohkura, Radiat. Eff. Defects Solids **134**, 345 (1995).
[44] N. Akiyama, P. Raerinne, H. Taketani, and H. Ohkura (unpublished).
[45] J.-M. Spaeth, J. R. Niklas, and R. H. Bartram, in *Structural Analysis of Point Defects in Solids* (Springer-Verlag, Heidelberg, 1993), pp. 273–275.
[46] K. Murayama, K. Morigaki, and H. Kanzaki, J. Phys. Soc. Jpn. **38**, 1623 (1975).
[47] A. C. Mezger and C. Jaccard, Solid State Commun. **41**, 301 (1982).
[48] P. A. Schnegg, C. Jaccard, and M. Aegerter, Phys. Status Solidi B **63**, 587 (1974).
[49] C. Jaccard, P. A. Schnegg, and M. Aegerter, Phys. Status Solidi B **70**, 485 (1975).
[50] L. F. Mollenauer, S. Pan, and S. Yngvesson, Phys. Rev. Lett. **23**, 683 (1969).
[51] Y. Ruedin, P. A. Schnegg, C. Jaccard, and M. Aegerter, Phys. Status Solidi B **54**, 565 (1972).
[52] A. Miehlich, Z. Phys. **176**, 168 (1963).
[53] H. Ohkura, K. Murakami, K. Iwamori, S. Nakamura, and Y. Mori, J. Phys. Soc. Jpn. **34**, 275 (1973).
[54] H. Ohkura, Bull. Okayama Univ. Sci. **29A**, 55 (1994).